

S. Munier\*

*Centre de physique théorique, École polytechnique, 91128 Palaiseau cedex, France<sup>†</sup>*

R. Peschanski<sup>‡</sup>

*Service de physique théorique, CEA/Saclay, 91191 Gif-sur-Yvette cedex, France<sup>§</sup>*

We propose a general method to study the solutions to nonlinear QCD evolution equations, based on a deep analogy with the physics of traveling waves. In particular, we show that the transition to the saturation regime of high energy QCD is identical to the formation of the front of a traveling wave. Within this physical picture, we provide the expressions for the saturation scale and the gluon density profile as a function of the total rapidity and the transverse momentum. The application to the Balitsky-Kovchegov equation for both fixed and running coupling constants confirms the effectiveness of this method.

## I. INTRODUCTION

Phenomenology of high energy deep-inelastic scattering in the framework of QCD leads to the study of evolution equations for the gluon distribution function  $\mathcal{N}(k, Y)$  at high density [1, 2, 3].  $Y$  is the rapidity of the evolved gluons and plays the rôle of the evolution variable, and  $k$  is their transverse momentum. The main feature of these evolution equations is that they contain nonlinear damping terms which make them difficult to solve by general methods. These damping terms reflect the effect of saturation, which is due to the recombination of partons densely packed together. The evolution at low density is well-understood and is described by a linear equation. The deep saturation regime can also be evaluated. However, the transition between these two regimes is still a challenge.

The purpose of the present paper is to propose a new method for handling this problem. It is based on a deep connection that we have found between the formation of traveling wave fronts in nonlinear physics and the transition to saturation.

We expect our method to be very general and applicable for different types of equations. In the present paper, we are going to apply it in detail to the Balitsky-Kovchegov (BK) equation [3], which reads

$$\partial_Y \mathcal{N} = \bar{\alpha} \chi(-\partial_L) \mathcal{N} - \bar{\alpha} \mathcal{N}^2, \quad (1)$$

where  $L = \log(k^2/\Lambda_{\text{QCD}}^2)$ . The QCD coupling  $\bar{\alpha}$  is either fixed or runs with  $k$ , in which case it is given by

$$\bar{\alpha}(L) = \frac{\alpha_s(L) N_c}{\pi} = \frac{1}{bL}, \quad b = \frac{11N_c - 2N_f}{12N_c}. \quad (2)$$

The function  $\chi$  is the well-known Balitsky-Fadin-Kuraev-Lipatov (BFKL) kernel [4]

$$\chi(\gamma) = 2\psi(1) - \psi(\gamma) - \psi(1 - \gamma) \quad (3)$$

and  $\chi(-\partial_L)$  is an integro-differential operator which may be defined with the help of the formal series expansion

$$\chi(-\partial_L) = \chi(\gamma_0) \mathbf{1} + \chi'(\gamma_0)(-\partial_L - \gamma_0 \mathbf{1}) + \frac{1}{2} \chi''(\gamma_0)(-\partial_L - \gamma_0 \mathbf{1})^2 + \frac{1}{6} \chi^{(3)}(\gamma_0)(-\partial_L - \gamma_0 \mathbf{1})^3 + \dots \quad (4)$$

for some given  $\gamma_0$  between 0 and 1, *i.e.* for the principal branch of the function  $\chi$ . The BK equation is expected to capture the main features of saturation effects in high energy scattering processes like virtual photon-nucleus (or proton under certain conditions) total cross section.

In a previous paper and in the case of fixed QCD coupling, we have already shown [5] the intimate connection between the limiting speed of a wave front and geometric scaling, namely the dependence of  $\mathcal{N}(k, Y)$  on a unique

<sup>†</sup> UMR 7644, unité mixte de recherche du CNRS.

<sup>§</sup> URA 2306, unité de recherche associée au CNRS.

\*Electronic address: Stephane.Munier@cpht.polytechnique.fr

<sup>‡</sup>Electronic address: pesch@spht.saclay.cea.fr

scaling variable  $k/Q_s(Y)$ , where  $Q_s$  is the so-called *saturation scale*. Interestingly enough, geometric scaling has been observed in the HERA data on inclusive  $\gamma^* - p$  scattering [6]. One aspect of the present letter is to go beyond these asymptotic results and to show how the approach to geometric scaling is related to the mechanism of wave front formation. This requires a method to get information on the form of the wave front when rapidity increases. Another goal is to extend our analysis to both fixed and running QCD coupling.

In Sec.II, we present the general method that we propose. In Sec.III, we treat the fixed coupling problem and in Sec.IV the running coupling one. For both cases we derive the expressions for the saturation scale  $Q_s(Y)$  and for the gluon density  $\mathcal{N}(k/Q_s(Y), Y)$  in the vicinity of the geometric scaling region  $L \sim \log(Q_s^2/\Lambda_{\text{QCD}}^2)$ . The final Sec.V is devoted to a discussion and summary.

## II. PHASE VELOCITY, GROUP VELOCITY AND WAVE FRONT FORMATION

Let us outline the method how to investigate traveling wave solutions to nonlinear partial derivative equations.

Our analysis comes from the physics of linearly unstable front equations of diffusion type. They appear *e.g.* for Rayleigh instabilities in hydrodynamical flows, directed polymers in random media, chemical and bacterial growth models etc... [7]. The evolution equations have the property to admit traveling wave solutions. Their existence is due to nonlinear damping while some of their large time characteristic features (front velocity, front shape) are determined by the *linearized* equation about the unstable state. The front is said to be “pulled” by this unstable state which appears as an unstable fixed point of the equation. The main rôle of the nonlinearities is to cause saturation.

Let us illustrate these features on the generic equation

$$\partial_t u(x, t) = \mathbb{D} \cdot u(x, t) + f(u) \quad (5)$$

where  $\mathbb{D}$  is a linear operator acting on functions of  $x$ ,  $f(u)$  contains the nonlinearities, with the requirement that  $\mathbb{D} \cdot u(x = \text{const.}, t) = 0$ , and  $f(0) = 0$ , so that  $u = 0$  is a fixed point. This fixed point is furthermore required to be unstable with respect to perturbations, which has to be checked in each particular case.

The simplest case is the Fisher and Kolmogorov-Petrovsky-Piscounov (KPP) equation [8] corresponding to  $\mathbb{D} = \partial_x^2$  and  $f(u) = u - u^2$ , for which rigorous mathematical results are available [9]. Using a change of variables, we have shown [5] that the BK equation reduces to the KPP equation when its kernel (3) is approximated by the first three terms of the expansion (4).

More generally, on physical grounds<sup>1</sup>, we expect the methods developed to treat the KPP equation to be valid for any saturation equation in QCD. Indeed, the common feature of these equations is that their nonlinearities cause saturation of the parton densities, and the fixed point of low gluon density is clearly linearly unstable under rapidity evolution. This instability is physically related to the growth of parton densities with rapidity given by the BFKL equation [4].

We shall study the form of the wave front at large times by working in its own reference frame which is defined by the change of variable  $x = x_{\text{WF}} + vt$ , and in the neighbourhood of the front, namely  $x_{\text{WF}} \ll vt$ . The velocity  $v$  of the wave front will be determined by consistency as the velocity of the slowest wave present in the initial wave packet.

The solution to the linear part of equation (5) corresponds to a linear superposition of waves:

$$u(x, t) = \int_{\mathcal{C}} \frac{d\gamma}{2i\pi} u_0(\gamma) \exp \{ -\gamma(x_{\text{WF}} + vt) + \omega(\gamma)t \} , \quad (6)$$

where  $\omega(\gamma)$  is the Mellin transform of the linear kernel ( $\partial_x^2 + 1$  for the KPP equation) and defines the dispersion relation of the linearized equation. In particular, each partial wave of wave number  $\gamma$  has a *phase velocity*

$$v_\varphi(\gamma) = \frac{\omega(\gamma)}{\gamma} \quad (7)$$

whose expression is found by imposing that the exponential factor in Eq.(6) be time independent for  $v = v_\varphi(\gamma)$ . By contrast, the *group velocity* is defined by the saddle point  $\gamma_c$  of the exponential phase factor

$$v = \left. \frac{d\omega}{d\gamma} \right|_{\gamma_c} \equiv v_g . \quad (8)$$

---

<sup>1</sup> At variance with the case of the KPP equation, mathematical proofs are lacking for properties of general nonlinear equations. However, a large number of results [7] have been found which *e.g.* numerically confirm the existence and properties of traveling wave solutions to equations of the type (5).

Let us show that the actual velocity  $v$  of the front depends on the competition between the singularities of  $u_0(\gamma)$  and the saddle point of the phase factor.

In Eq.(6),  $u_0(\gamma)$  is the initial condition in Mellin space, *i.e.* the Mellin transform of  $u(x, t=0)$ . The physically appropriate assumption is that  $u_0(\gamma)$  is a monotoneous function smoothly connecting 1 to 0 as  $x$  goes from  $-\infty$  to  $+\infty$ , with asymptotic behavior  $u(x, t=0) \sim e^{-\gamma_0 x}$  [5]. Then  $u_0(\gamma)$  has singularities on the real axis starting at 0 and extending to the left, and at  $\gamma_0$  to the right. A simple case study is  $u(0, x) = 1$  for  $x \leq 0$  and  $u(0, x) = e^{-\gamma_0 x}$  for  $x > 0$ , whose exact Mellin transform is  $u_0(\gamma) = 1/\gamma + 1/(\gamma_0 - \gamma)$ . The contour  $\mathcal{C}$  in (6) runs parallel to the imaginary axis and crosses the real axis at a point between 0 and  $\gamma_0$ . There are three relevant cases (see Fig.1):

(i)  $\gamma_0 < \gamma_c$ : dominance of initial conditions. The integral (6) defining  $u$  is dominated by the pole at  $\gamma_0$ , thus  $u \sim \exp\{-\gamma_0(x_{\text{WF}} + vt) + \omega(\gamma_0)t\}$  and the velocity of the front is determined by consistency to be  $v \equiv \omega(\gamma_0)/\gamma_0$ , which ensures the time-independence in the reference frame of the front.

(ii)  $\gamma_0 > \gamma_c$ : dominance of the saddle point. The integral in Eq.(6) is now  $\sim \exp\{-\gamma_c(x_{\text{WF}} + vt) + \omega(\gamma_c)t\}$  and thus the velocity  $v$  of the front is defined by

$$v = v_g = \frac{\omega(\gamma_c)}{\gamma_c} = \min_{\gamma} \frac{\omega(\gamma)}{\gamma} . \quad (9)$$

Indeed, in this case, the group velocity is identical to the minimum of the phase velocity. In the previous case instead, the front velocity is  $v = \omega(\gamma_0)/\gamma_0 > v_g$ .

(iii)  $\gamma_0 = \gamma_c$ : critical case. Both the pole and the saddle point contribute, and  $v = v_g$ .

Now that we have determined the velocity of the wave front, reporting it in Eq.(6) and performing the integral in the large  $t$  limit gives the asymptotic expression for the form of the front:

$$u(x, t) \underset{t \rightarrow \infty}{\sim} \begin{cases} e^{-\gamma_0 x_{\text{WF}}} & \text{if } \gamma_0 < \gamma_c \\ e^{-\gamma_c x_{\text{WF}}} & \text{if } \gamma_0 \geq \gamma_c \end{cases} . \quad (10)$$

The typical wave front solutions are illustrated on Fig.2. The upper plot displays a typical feature of the wave front development for the case  $\gamma_0 < \gamma_c$ . Here the front moves with the velocity  $v_- > v_g$  and keeps the memory of the initial condition. The lower plot illustrates the case  $\gamma_0 > \gamma_c$ . In this case, the wave front develops with the fixed group velocity  $v_g$ . The forward part of the curve (after the knee) is the part of the front which keeps the memory of the initial condition, which is a typical feature of a “pulled” front [7]. The middle plot is for the critical case  $\gamma_0 = \gamma_c$ .

In the following, we will focus on the case in which the initial condition is steep enough, so that the velocity of the front is the group velocity (8) and the form of the wave front is the second equation of (10).

It is interesting for our purpose to go beyond the asymptotics (10) and study how the front reaches its asymptotic form as a function of time. For this sake, we shall use the following ansatz in the neighbourhood of the front:

$$u(x, t) \underset{t \text{ large}}{=} t^\alpha G\left(\frac{x_{\text{WF}} + c(t)}{t^\alpha}\right) e^{-\gamma_c(x_{\text{WF}} + c(t))} , \quad (11)$$

where  $c(t)$  is a subdominant function of time (with respect to  $v_g t$ ). Indeed, the front velocity receives some sub-asymptotic corrections w.r.t. the constant asymptotic velocity  $v_g$ , contained in the derivative  $\dot{c}(t) = dc(t)/dt$ . The factors  $t^\alpha$  describe a diffusion-like evolution which will be made explicit in each particular case. Hence the function  $t^\alpha G$  represents a subasymptotic correction to the form of the front (10) at large times. This ansatz was proven to be relevant for KPP-like equations [10]. Its key property is to be a solution of the linearized equation at large  $t$  in the neighbourhood of the front, for some  $\alpha$  and  $c(t)$  to be determined. Note that since  $u(x, t)$  only depends on  $x_{\text{WF}} + c(t)$  when the front has reached its asymptotic form of a pure traveling wave,  $G(z)$  is required to vanish like  $z$  for  $z \rightarrow 0$ .

The features of this ansatz are displayed on the lowest plot in Fig.2. One sees that a steep initial condition characterized by the exponential decay slope  $\gamma_0$  evolves, after a given time  $t$ , into a front characterized by the critical exponential decay slope  $\gamma_c$ . Its width is of order  $t^\alpha$  as we will show later on.

### III. BK EQUATION WITH FIXED QCD COUPLING

Let us first apply the formalism exposed above to the BK equation with fixed coupling  $\bar{\alpha}$ . The linear part of Eq.(1) is solved by

$$\mathcal{N}(k, Y) = \int \frac{d\gamma}{2i\pi} \mathcal{N}_0(\gamma) \exp(-\gamma L + \bar{\alpha}\chi(\gamma)Y) . \quad (12)$$

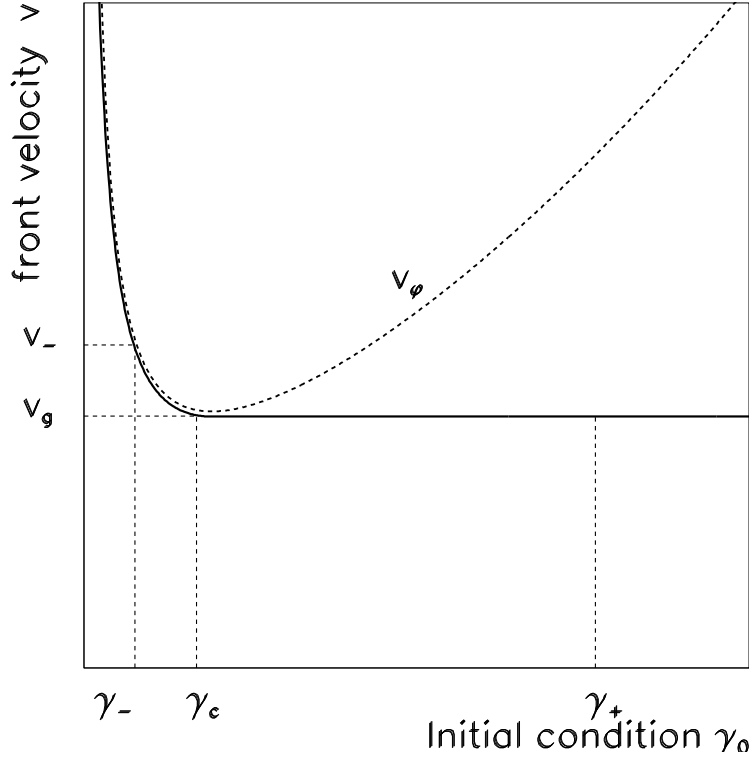


FIG. 1: The front velocity as a function of the steepness  $\gamma_0$  of the initial condition at  $x \rightarrow \infty$  ( $u(x, t=0) \sim e^{-\gamma_0 x}$ ). *Continuous line*: the actual front velocity. *Dashed line*: the phase velocity for a wave with wave number  $\gamma_0$ . The abscissa points  $\gamma_-$ ,  $\gamma_+$ ,  $\gamma_c$  correspond to initial conditions resp. below, larger than and equal to the critical value (resp. cases (i), (ii) and (iii), see text).

The rapidity  $Y$  is the evolution variable, and thus plays the rôle of the time  $t$ , while  $L = \log(k^2/\Lambda_{\text{QCD}}^2)$  plays the rôle of the spatial coordinate  $x$ .

Let us discuss the relevant initial condition  $\mathcal{N}_0(\gamma)$  for QCD. The essential property for the derivation is that at large  $L$  (*i.e.* large  $k$ ),  $\mathcal{N}(k, Y=0) \sim k^{-2}$ : this corresponds to the color transparency property of gauge theories, and yields  $\gamma_0 = 1$ . For  $L$  small or negative, the dynamics is unknown since it belongs to the nonperturbative regime of QCD. However, interestingly enough, it does not play a direct rôle in the final result for the front formation. One may assume that  $\mathcal{N}(k, Y=0)$  is bounded [5], which is a way to impose unitarity on the initial condition. In Mellin space, this leads to singularities of  $\mathcal{N}_0(\gamma)$  distributed on the intervals  $]-\infty, 0]$  and  $[1, +\infty[$ . We shall verify in a moment that the wave number  $\gamma_c$  which minimizes the *phase velocity*, *i.e.* the wave number of the partial wave which moves with the *group velocity*, is between 0 and 1. Thus we are in the case (ii) of Sec.II in which the saddle point dominates.

We shall now proceed to the determination of the analogous of the group velocity  $v_g$ . By comparison of Eq.(12) to Eq.(6), one sees that the dispersion relation reads

$$\omega(\gamma) = \bar{\alpha}\chi(\gamma) . \quad (13)$$

The phase velocity  $v_\phi(\gamma) = \omega(\gamma)/\gamma$  has a minimum at  $\gamma_c$ . From Eqs.(8,9),  $\gamma_c$  solves the implicit equation

$$\gamma_c \chi'(\gamma_c) = \chi(\gamma_c) , \quad (14)$$

which yields  $\gamma_c = 0.6275\dots$ . This number indeed stands between 0 and 1, and thus we are in a similar situation as the one depicted on the third plot of Fig.2: the front velocity is blocked at the value

$$v_g = \bar{\alpha} \frac{\chi(\gamma_c)}{\gamma_c} . \quad (15)$$

To study the formation of the front, we will stick to the “diffusive” approximation of the BK equation (1), defined

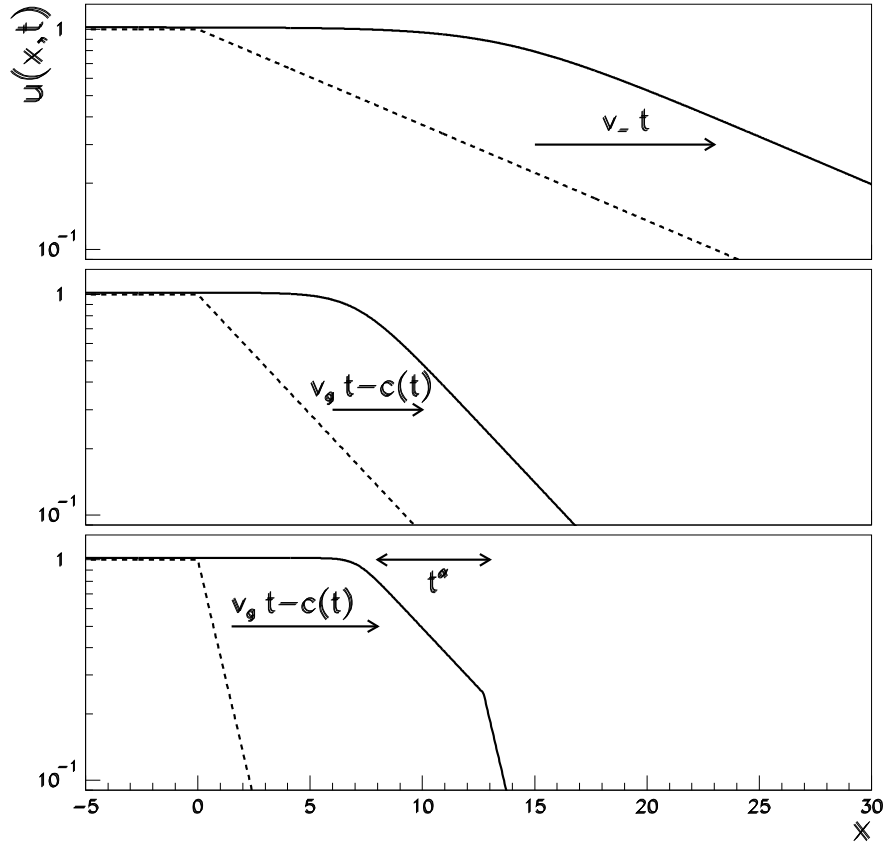


FIG. 2: Picture of the evolution of a front for three typical initial conditions. *Dashed line*: the initial profile  $u(x, t = 0)$ . *Full line*: the evolved front after at large time  $t$ . *Upper plot* (case (i)): the exponential slope  $\gamma_0$  of the initial condition is  $\gamma_- < \gamma_c$ . The front propagates at the phase velocity  $v_- = v_\varphi(\gamma_-)$ . *Middle plot* (case (iii)):  $\gamma_0 = \gamma_c$ . The front propagates at velocity  $v_g$ . *Lower plot* (case (ii)):  $\gamma_0 = \gamma_+ > \gamma_c$ . The front still propagates at velocity  $v_g$ , the size of the front is finite of order  $t^\alpha$ , and its slope is given by  $\gamma_c$ .

by keeping terms up to the second order only in the expansion (4):

$$\chi(-\partial_L) = \chi(\gamma_c) + (-\partial_L - \gamma_c \mathbf{1})\chi'(\gamma_c) + \frac{1}{2}(-\partial_L - \gamma_c \mathbf{1})^2\chi''(\gamma_c). \quad (16)$$

Within this approximation, the nonlinear equation becomes

$$\partial_Y \mathcal{N} = -v_g \partial_L \mathcal{N} + \frac{1}{2} \bar{\alpha} \chi''(\gamma_c) (\partial_L + \gamma_c \mathbf{1})^2 \mathcal{N} - \bar{\alpha} \mathcal{N}^2, \quad (17)$$

which is equivalent to the KPP equation [5].

We now use the ansatz (11) as the appropriate solution of the linearized version of Eq.(17) near the wave front. Setting  $u = \mathcal{N}$ ,  $x = L$  and  $t = Y$ , the linear part of Eq.(17) turns into an ordinary differential equation for  $G(z)$ , namely

$$\frac{1}{2} \bar{\alpha} \chi''(\gamma_c) Y^{-\alpha} G''(z) + (\alpha z Y^{\alpha-1} - \dot{c}(Y)) G'(z) + Y^{\alpha-1} (\gamma_c \dot{c}(Y) Y - \alpha) G(z) = 0 \quad (18)$$

where  $z$  is related to the physical variables through

$$z \equiv \frac{x_{\text{WF}} + c(t)}{t^\alpha} = \frac{(L - v_g Y) + c(Y)}{Y^\alpha}. \quad (19)$$

The different terms in Eq.(18) contribute equally if  $\alpha = \frac{1}{2}$  and  $\dot{c}(Y) = \beta/Y$ , where  $\beta$  is a constant. This value of  $\alpha$  ensures that the terms proportional to  $Y^{-\alpha}$  and  $Y^{\alpha-1}$  contribute to the same order in  $Y$ . Using these values, Eq.(18) boils down to a simple second order differential equation

$$\frac{1}{2}\bar{\alpha}\chi''(\gamma_c)G''(z) + \frac{1}{2}zG'(z) + (\beta\gamma_c - \frac{1}{2})G(z) = 0 . \quad (20)$$

The constant  $\beta$  is determined by requiring that  $G$  behave smoothly for  $z \rightarrow +\infty$ , which fixes uniquely<sup>2</sup>  $\beta = 3/(2\gamma_c)$  [10]. The solution which vanishes at  $z = 0$  is unique up to a constant and reads

$$G(z) = \text{const.} \times \sqrt{\frac{2}{\bar{\alpha}\chi''(\gamma_c)}} z \exp\left(-\frac{z^2}{2\bar{\alpha}\chi''(\gamma_c)}\right) . \quad (21)$$

In terms of physical variables, the gluon density near the wave front thus reads

$$\mathcal{N}(k/Q_s(Y), Y) = \text{const.} \times \sqrt{\frac{2}{\bar{\alpha}\chi''(\gamma_c)}} \log\left(\frac{k^2}{Q_s^2(Y)}\right) \left(\frac{k^2}{Q_s^2(Y)}\right)^{-\gamma_c} \exp\left(-\frac{1}{2\bar{\alpha}\chi''(\gamma_c)Y} \log^2\left(\frac{k^2}{Q_s^2(Y)}\right)\right) \quad (22)$$

with the saturation scale defined as

$$Q_s^2(Y) = Q_0^2 \exp\left(\bar{\alpha}\frac{\chi(\gamma_c)}{\gamma_c}Y - \frac{3}{2\gamma_c}\log Y\right) . \quad (23)$$

$Q_0$  absorbs undetermined constants but remains of order  $\Lambda_{\text{QCD}}$ . Note that (23) reproduces the result of [5] after expansion of  $\gamma_c$  around  $\frac{1}{2}$ .

#### IV. BK EQUATION WITH RUNNING QCD COUPLING

We turn to the case in which the coupling in Eq.(1) runs with  $L$  as given by Eq.(2). The BK equation reads

$$bL \partial_Y \mathcal{N} = \chi(-\partial_L) \mathcal{N} - \mathcal{N}^2 , \quad (24)$$

with  $b$  defined in Eq.(2). Using a double Mellin transform, the linearized version of the equation gives the solution

$$\mathcal{N}(k, Y) = \int \frac{d\gamma}{2i\pi} \int \frac{d\omega}{2i\pi} \mathcal{N}_0(\gamma, \omega) \exp\left(-\gamma L + \omega Y + \frac{1}{b\omega} X(\gamma)\right) , \quad (25)$$

where

$$X(\gamma) = \int_{\hat{\gamma}}^{\gamma} d\gamma' \chi(\gamma') . \quad (26)$$

At this stage,  $\hat{\gamma}$  is an undetermined constant. The initial condition  $\mathcal{N}_0(\gamma, \omega)$  depends now both on  $\omega$  and  $\gamma$ , but has to satisfy the same requirements as in the fixed coupling case (color transparency at large  $k$ , saturation at smaller  $k$ ) resulting in a specific analytic structure in  $\gamma$  as already discussed in Sec.III.

Performing the integral over  $\omega$  in the large  $Y$  limit, the integral is dominated by a saddle point at  $\omega_c = \sqrt{bX(\gamma)/Y}$ . The solution reads

$$\mathcal{N}(L, Y) = \int \frac{d\gamma}{2i\pi} \mathcal{N}_0(\gamma) \exp\left(-\gamma L + \sqrt{Y} \sqrt{\frac{4X(\gamma)}{b}}\right) , \quad (27)$$

where  $\mathcal{N}_0(\gamma)$  keeps track of all prefactors. Now interpreting  $\sqrt{Y}$  as the time variable  $t$ , the gluon density turns out to be also a linear superposition of traveling waves labelled by  $\gamma$ , and thus can be treated by the general method exposed in Sec.II. In this case, the asymptotic dispersion relation is

$$\omega(\gamma) \equiv \sqrt{\frac{4X(\gamma)}{b}} . \quad (28)$$

---

<sup>2</sup> The full asymptotics of  $G$  in the framework of the KPP equation can be found in Ref.[10].

The minimum  $\bar{\gamma}$  of  $v_\varphi(\gamma) = \omega(\gamma)/\gamma$  satisfies the equation

$$2X(\bar{\gamma}) = \bar{\gamma} \chi(\bar{\gamma}) , \quad (29)$$

still depending at this stage on the choice of  $\hat{\gamma}$  in Eq.(26). The velocity of the front (see Eq.(8)) is given by

$$v_g = \sqrt{\frac{2\chi(\bar{\gamma})}{b\bar{\gamma}}} . \quad (30)$$

Requiring the velocity  $v_g$  to become independent of the choice of  $\hat{\gamma}$  leads to the constraint  $dv_g(\hat{\gamma})/d\hat{\gamma} = 0 = dv_g(\bar{\gamma})/d\bar{\gamma}$ , namely

$$\bar{\gamma} \chi'(\bar{\gamma}) = \chi(\bar{\gamma}) . \quad (31)$$

The comparison with Eq.(14) shows that  $\bar{\gamma}$  is identical to  $\gamma_c = 0.6275\dots$ , the critical wave number in the non-running case, and thus the velocity of the front reads

$$v_g = v(\gamma_c) = \sqrt{\frac{2\chi(\gamma_c)}{b\gamma_c}} . \quad (32)$$

Once the asymptotic velocity is known, we compute the transition to saturation through subleading corrections to  $v_g$ . To this aim, one expands the linearized BK equation around  $\gamma_c$  to get

$$\frac{bL}{2t} \partial_t \mathcal{N} = -\frac{bv_g^2}{2} \partial_L \mathcal{N} + \frac{\chi''(\gamma_c)}{2} (\partial_L^2 \mathcal{N} + 2\gamma_c \partial_L \mathcal{N} + \gamma_c^2 \mathcal{N}) . \quad (33)$$

One uses the ansatz (11) for the solution to this equation at large  $t$ , which turns it into an ordinary second order differential equation. After tedious but straightforward compilation of all terms, one determines the coefficient  $\alpha$  and the function  $c(t)$  by requiring that they all contribute equally. One finds  $\alpha = \frac{1}{3}$  and  $\dot{c}(t) = \beta t^{-2/3}$ , where  $\beta$  still needs to be fixed. The value of  $\alpha$  comes from keeping relevant terms in  $Y^{-\alpha}$  and  $Y^{2\alpha-1}$ , which all contribute at large  $Y$ .

Finally, Eq.(33) reduces to the Airy equation

$$G''(z) = \frac{b\gamma_c v_g}{\chi''(\gamma_c)} (z - 4\beta) G(z) . \quad (34)$$

There are two independent solutions to this equation, *e.g.* Ai and Bi. Imposing the regularity at  $z = +\infty$  selects

$$G(z) = \text{const.} \times \text{Ai} \left( \left( \frac{\gamma_c v_g b}{\chi''(\gamma_c)} \right)^{1/3} (z - 4\beta) \right) . \quad (35)$$

The condition  $G(z) \sim z$  for small  $z$  is satisfied if

$$\beta = -\frac{1}{4} \left( \frac{\chi''(\gamma_c)}{\gamma_c v_g b} \right)^{1/3} \xi_1 , \quad (36)$$

where  $\xi_1 = -2.338\dots$  is the rightmost zero of the Airy function. The complete result reads, in physical variables

$$\mathcal{N}(k/Q_s(Y), Y) = \text{const.} \times Y^{1/6} \left( \frac{k^2}{Q_s^2(Y)} \right)^{-\gamma_c} \text{Ai} \left( \xi_1 + \left( \frac{\sqrt{\gamma_c \chi(\gamma_c) b}}{\chi''(\gamma_c)} \right)^{1/3} \frac{\log(k^2/Q_s^2(Y))}{Y^{1/6}} \right) , \quad (37)$$

where the saturation scale is given by

$$Q_s^2(Y) = \Lambda_{\text{QCD}}^2 \exp \left( \sqrt{\frac{2\chi(\gamma_c)}{b\gamma_c}} Y + \frac{3}{4} \left( \frac{\chi''(\gamma_c)}{\sqrt{\gamma_c \chi(\gamma_c) b}} \right)^{1/3} \xi_1 Y^{1/6} \right) , \quad (38)$$

up to a multiplicative constant.

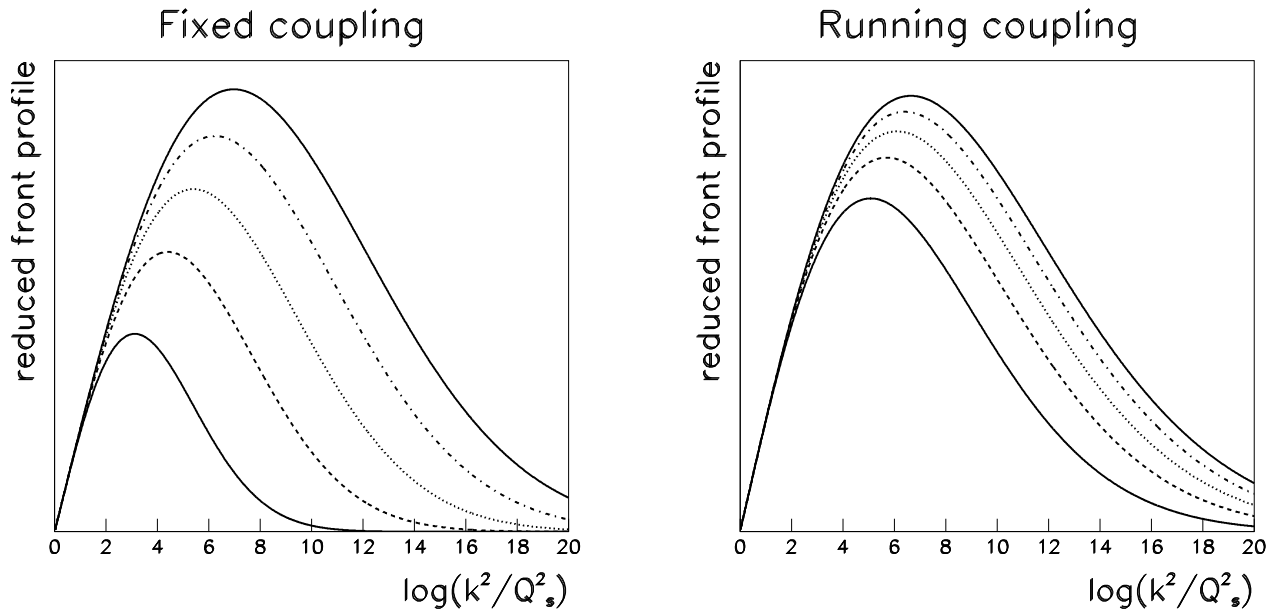


FIG. 3: Evolution of the reduced front profile in the case of fixed coupling (left) and running coupling (right). The reduced front profile  $(k^2/Q_s^2)^{\gamma_c} \mathcal{N}(k/Q_s(Y), Y)$  is plotted against  $\log(k^2/Q_s^2)$  for different rapidities. The various lines correspond to rapidities from 2 (lower curves, full line) up to 10 (upper curves). Note the similarity of the wave fronts, but the quicker time evolution (in  $\sqrt{t}$ ) for fixed coupling, by contrast with the slow time evolution (in  $t^{1/3}$ ) for the running coupling case.

## V. DISCUSSION AND CONCLUSION

Let us discuss our final results for fixed (22,23) and running (37,38) coupling. In both cases, we get the leading exponential terms (resp.  $\bar{\alpha}(\chi(\gamma_c)/\gamma_c)Y$  and  $\sqrt{2(\chi(\gamma_c)/b\gamma_c)Y}$ ) in the expressions for the saturation scale found in Refs.[11, 12]. These terms are supplemented by subleading corrections in rapidity, which are precisely those present in Ref.[12], and which are respectively proportional to  $\log Y$  and  $Y^{1/6}$ . They are related to the slowing down of the velocity due to formation of the wave front. We expect this slowing down to be a very general feature of the transition to saturation. The expressions for the front profiles exhibit geometric scaling violations which are due to the time (*i.e.* rapidity) delay for the formation of the front.

Comparing to the results which were obtained from the linear evolution equation supplemented by absorptive boundary conditions [12], we have confirmed these results for the running coupling case, up to a constant multiplicative factor in the definition of the saturation scale  $Q_s$ . For the fixed coupling case, the same is true within the geometric scaling region  $k \sim Q_s(Y)$ . Our formula (22) provides a hint on the geometric scaling violations. Note that an extension to the next-to-leading order BFKL kernel has been found in Ref.[13]. It would be interesting to see whether this result can also be obtained by our method.

To summarize, in this paper, we have proposed a general method, physically appealing, which allows to determine both the saturation scale and the transition of the gluon density towards saturation for the solution of the Balitsky-Kovchegov nonlinear equation. The method is based on a direct analogy with traveling wave solutions of nonlinear equations of the KPP type. The saturation scale is related to the velocity of the wave front, and the transition to saturation of the gluon distribution to the diffusive type formation of the front. In particular, we have studied directly the solution to the nonlinear equation, instead of assuming specific boundary conditions on the linear one.

As first applications of this method, using a general ansatz [10], we have derived in a rather simple way the physical solutions to the BK equation at large rapidity for both fixed and running coupling, see Eqs.(22,23) and (37,38). The approach to saturation (leading to geometric scaling violations) corresponds to ordinary diffusion (namely with a diffusion length going like  $\sqrt{t}$ ) in the fixed coupling case and to anomalous diffusion (in  $t^{1/3}$ ) in the running coupling case. These contrasted diffusion patterns towards saturation are made explicit in the evolution of the reduced front profile  $(k^2/Q_s^2)^{\gamma_c} \mathcal{N}(k/Q_s(Y), Y)$  shown on Fig.3.

We think that the method that we have presented is general enough to allow for desirable extensions to the full content of saturation equations.

We thank Bernard Derrida for his illuminating advices on traveling waves and KPP-like equations.

- 
- [1] L.V. Gribov, E.M. Levin and M.G. Ryskin, Phys. Rep. **100**, 1 (1983); A.H. Mueller, J. Qiu, Nucl. Phys. **B268**, 427 (1986).
  - [2] L. McLerran and R. Venugopalan, Phys. Rev. **D49**, 2233 (1994); *ibid.*, 3352 (1994); *ibid.*, **D50**, 2225 (1994); A. Kovner, L. McLerran and H. Weigert, Phys. Rev. **D52**, 6231 (1995) ; *ibid.*, 3809 (1995); R. Venugopalan, Acta Phys.Polon. **B30**, 3731 (1999); E. Iancu, A. Leonidov, and L. McLerran, Nucl. Phys. **A692**, 583 (2001); *idem*, Phys. Lett. **B510**, 133 (2001); E. Iancu and L. McLerran, Phys. Lett. **B510**, 145 (2001); E. Ferreira, E. Iancu, A. Leonidov and L. McLerran, Nucl. Phys. **A703**, 489 (2002); H. Weigert, Nucl. Phys. **A703**, 823 (2002).
  - [3] I. Balitsky, Nucl. Phys. **B463**, 99 (1996); Y. V. Kovchegov, Phys. Rev. **D60**, 034008 (1999); *ibid.*, **D61**, 074018 (2000).
  - [4] L. N. Lipatov, Sov. J. Nucl. Phys. **23**, 338 (1976); E. A. Kuraev, L. N. Lipatov, and V. S. Fadin, Sov. Phys. JETP **45**, 199 (1977); I. I. Balitsky and L. N. Lipatov, Sov. J. Nucl. Phys. **28**, 822 (1978).
  - [5] S. Munier and R. Peschanski, “*Geometric scaling as traveling waves*”, to appear in Phys. Rev. Lett., [arXiv:hep-ph/0309177].
  - [6] A. M. Staśto, K. Golec-Biernat, and J. Kwiecinski, Phys. Rev. Lett. **86**, 596 (2001).
  - [7] Wim van Saarloos, Phys. Rep. **386**, 29 (2003).
  - [8] R. A. Fisher, Ann. Eugenics **7**, 355 (1937); A. Kolmogorov, I. Petrovsky, and N. Piscounov, Moscou Univ. Bull. Math. **A1**, 1 (1937).
  - [9] M. Bramson, Memoirs of the American Mathematical Society **285** (1983).
  - [10] E. Brunet and B. Derrida, Phys. Rev. **E56**, 2597 (1997) and references therein.
  - [11] E. Iancu, K. Itakura and L. McLerran, Nucl. Phys. A **708**, 327 (2002).
  - [12] A. H. Mueller and D. N. Triantafyllopoulos, Nucl. Phys. **B640**, 331 (2002).
  - [13] D. N. Triantafyllopoulos, Nucl. Phys. **B648**, 293 (2003).